ARTICLE

Check for updates

Varied response of carbon dioxide emissions to warming in oxic, anoxic and transitional soil layers in a drained peatland

Liangfeng Liu [1,2], Huai Chen [1,3✉] & Jianqing Tian [4]

Peatlands are an important natural store of carbon. Here, we investigate how carbon dynamics in soils from three distinct layers from a drained peatland in the Qinghai-Tibet Plateau might respond to global warming. We incubated Zoige Plateau soil samples that represent oxic surface soil, permanently waterlogged anoxic deep soil, and a transitional interlayer, which varies between oxic and anoxic conditions with water table fluctuations, in the laboratory at 8 °C and 18 °C for 154 days. We find that carbon quality and microbial activity were highest in surface soils and lowest in interlayer soils. Carbon dioxide emissions were lowest in interlayer soils, where they were less sensitive to warming and more sensitive to nitrogen content than in the other layers. Conversely, carbon quality and microbial activity were the primary predictors of carbon dioxide emissions from the surface and deep soil, respectively. Our findings suggest a low vulnerability of soil carbon in interlayer soils of drained peatlands to warming.

[1] CAS Key Laboratory of Mountain Ecological Restoration and Bioresource Utilization & Ecological Restoration and Biodiversity Conservation Key Laboratory of Sichuan Province, Chengdu Institute of Biology, Chinese Academy of Sciences, Chengdu 610041, China. [2] Zoige Peatland and Global Change Research Station, Chinese Academy of Sciences, Hongyuan 624400, China. [3] CAS Center for Excellence in Tibetan Plateau Earth Sciences, Chinese Academy of Sciences (CAS), Beijing 100101, China. [4] State Key Laboratory of Vegetation and Environmental Change, Institute of Botany, Chinese Academy of Sciences, Beijing 100093, China. ✉email: chenhuai@cib.ac.cn

Peatlands make up a critical part of the world's carbon pool, storing about 600 Pg carbon and covering 15–30% of the terrestrial biosphere[1]. However, against the background of continuous climate change and human activities, 15% of worldwide peatlands have been drained[2,3]. The CO_2 release from drained peatlands should be a high priority to investigate, because it contributes about 5% of the global anthropogenic CO_2 release[4], and has been considered the most important source of atmospheric CO_2[3].

Compared with pristine peatlands, the water table, which is one of the primary regulators of peat carbon accumulation[5], severely reduces in drained peatlands[4]. Water table drawdown exposes peatlands profile into three layers with distinct hydrological and oxygenation characteristics: surface soil is predominantly oxic and contains living plants and roots; deep soil is perpetually waterlogged and anoxic, and lacks plant roots; and the interlayer between surface and deep soil alternates between being oxic and anoxic during water table fluctuation[6–8]. Long-term of these distinct characteristics lead to separations in soil biochemistry[6], which altogether may translate to different soil CO_2 release under climate change. However, the CO_2 release from these three layers of drained peatlands still remains unclear, because the stratification of the vertical profile in previous research of drained peatlands is two and is based on depth, like soil 20[9], 25[10], or 30 cm below the surface[11,12], neglecting the interlayer (Fig. 1). These considerations highlight the need to enclose the interlayer to clarify the magnitude and determinants of CO_2 release from drained peatlands.

The distribution of carbon quality[13,14] and microbes[9,15–17] are reported as two primary factors regulating the magnitude of CO_2 release. The study reports that carbon quality[18] and microbial activity always decrease with depth, because surface soil contains abundant labile carbon and nutrients from plants[19], whereas long-term decay leads to the accumulation of recalcitrant/inaccessible carbon in deep soil[18,20]. However, this simplistic assumption may not always hold for drained peatlands, because several studies find that carbon at the interlayer is most degraded during water table rise and fall[6,21].

The rise and fall of the water table may also complicate the distribution of microbes since they are regulated by carbon accessibility[22] and sensitive to local environmental changes[23–25]. For example, labile carbon like dissolved organic carbon (DOC) and water-soluble phenolics (H_2O-PHE) are easily accessible to

microbes[26,27] and enzymes[28], however, mineral-bound organic carbon is inaccessible to microbes[29,30]. Water table fluctuation can also create oxic-anoxic cycles at the interlayer that affect microbial metabolism pathways and activity. The potential for different carbon quality and microbial activity across the layers of drained peatlands implies that the layers should be analyzed separately in order to predict the carbon stability of drained peatlands.

Moreover, nitrogen (N) nutrition is becoming vital in regulating soil organic carbon (SOC) decomposition against the background of increasing N deposited[31]. Soil N could originate from plants or be released from soil aggregates or carbon macromolecules by microbes[32]. Research shows that the available N could significantly increase SOC decomposition and CO_2 release in arctic soils[33], due to N is necessary for microbes to produce extracellular enzymes that decompose soil carbon to get energy[16,34]. Therefore, any models of CO_2 release in water table-dependent soil layers must take nitrogen into account.

The distribution of carbon, microbial activity, and nitrogen nutrient also regulate the response of CO_2 release to climate warming. In a five years whole-soil warming experiment in a mixed coniferous forest, a study suggests that carbon loss is driven by the increases in microbial activity and DOC content[35], and in a decade warming experiment in a tallgrass prairie, the shift in microbial communities is reported largely associated with soil carbon loss[15]. The response of CO_2 release to warming in subtropical peatlands depends strongly on carbon quality and nutrient status[13], while the response of permafrost peatlands depends strongly on carbon quality in the surface layer but microbial activity in the deep layer[36]. These results greatly advance our knowledge of the determinant of CO_2 loss under a warming climate. However, the relative importance of the determinants across the soil profile, especially with respect to the water table, is unknown. To integrate these various determinants of CO_2 release into coherent climate models, we should examine them for the separate layers of drained peatlands.

Here, we examined the magnitude and determinants of CO_2 release from the three water table-dependent soil layers in a drained peatland on the Zoige plateau under a simulated warming climate (Supplementary Fig. 1). We explored the distribution of carbon and microbial composition in the three layers and quantified the magnitude of CO_2 release under warming conditions. We hypothesized that (1) carbon quality, microbial diversity, and CO_2 release would be lowest at the interlayer because of a periodically oxic decomposition during water table fluctuation[6]; (2) CO_2 release at the surface would depend primarily on microbial and enzyme activity, and CO_2 release from deep soil would depend primarily on carbon quality; (3) CO_2 release from the interlayer would be primarily regulated by nitrogen because the severe disturbance during water table fluctuation. We found that the CO_2 release in the interlayer is stable and less vulnerable to warming than at the surface or deep soil. The CO_2 released from the surface and deep soil are primarily controlled by carbon quality and decomposers, respectively. And the CO_2 release from the interlayer was sensitive to nitrogen variation.

Results

Carbon degradation indexes and chemical composition. Soil carbon degradation indexes, including C/N ratio, ash content, bulk density, $\delta^{13}C$, and $\delta^{15}N$ were shown in Supplementary Fig. 4. The C/N ratio was lower at the surface than the deeper two layers. Ash content and bulk density were significantly higher at the surface than in the other two layers. Deep soil showed the highest $\delta^{13}C$ and lowest $\delta^{15}N$ of the three layers.

SOC was higher at the interlayer and deep soil than the surface (Supplementary Fig. 4). The SOC composition as acquired by Solid-State ^{13}C CPMAS differed in certain respects among the
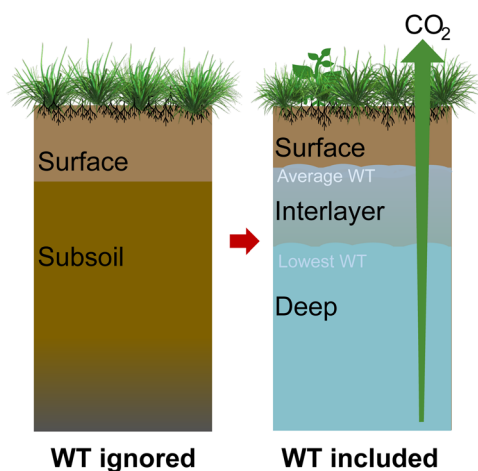
Fig. 1 Carbon release from the profile of drained peatlands. Previous research focused on absolute depth, neglecting the effects of water table fluctuations, which divided soil profile into three layers: oxic surface, oxic-anoxic transitional interlayer, and anoxic deep (WT water table).
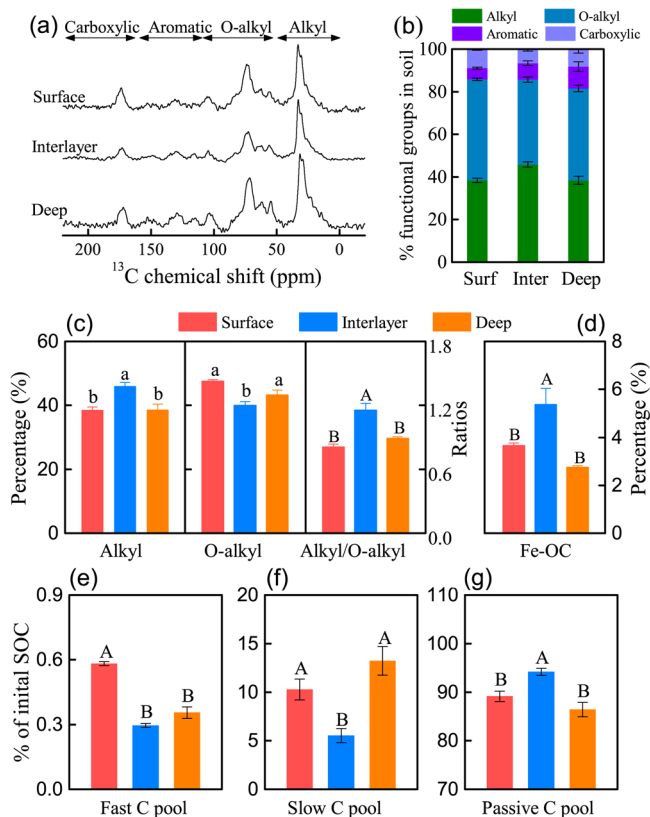
Fig. 2 Comparison of carbon composition, mineral-protected organic carbon, and carbon pool sizes in the three water table-dependent soil layers. a ^{13}C CPMAS NMR spectra. The following forms of carbon were analyzed in the spectra: alkyl-C, chemical shifts of 0–50 ppm; O-alkyl-C, 50–110 ppm; aromatic-C, 110–165 ppm; and carboxylic C, 165–220 ppm. **b** Relative percentages of the four forms of carbon relative to total SOC. Surf surface, Inter interlayer. **c** Percentages of alkyl-C or O-alkyl-C and the ratio of alkyl-C to O-alkyl-C. Percentages are plotted on the left vertical axis and ratios on the right vertical axis. **d** Percentage of Fe-bound organic carbon (Fe-OC). **e–g** three carbon pool size. Error bars denote SE ($n = 3$). Uppercase letters, $p < 0.01$; lowercase letters, $p < 0.05$ (Tukey HSD test). SOC soil organic carbon.

three layers. The proportion of alkyl-C was significantly higher at the interlayer (45.8%) than at the surface (38.4%) or deep soil (38.1%; both $p < 0.05$). Conversely, the proportion of O-alkyl-C (39.8%) was significantly lower at the interlayer than at the surface (47.5%) or deep soil (43.2%; both $p < 0.05$). The calculated alkyl/O-alkyl ratio was thus significantly higher at the interlayer than surface or deep soil ($p < 0.01$), indicating greater recalcitrant carbon in the interlayer soil (Fig. 2a–c). The three soil layers did not differ significantly in proportions of aromatic or carboxylic C (Supplementary Fig. 5). Fe-bound organic carbon (Fe-OC), which could reflect soil organic carbon protection by minerals was 1.5-1.9 times higher at the interlayer than the other two layers ($p < 0.01$; Fig. 2d).

The carbon composition of three layers of soil was further confirmed by the size of the carbon fraction pool (Fig. 2e–g). The fast carbon pool was significantly larger at the surface than in the other two layers ($p < 0.01$; Fig. 2e), and the slow carbon pool was significantly smaller in the interlayer than in the other two layers (Fig. 2f). Conversely, the passive carbon pool was significantly larger in the interlayer than in the other two layers (Fig. 2g).

Labile carbon levels also differed among the three layers. DOC was lowest at the surface and highest in the deep soil, while H_2O-PHE was lowest at the surface and highest in the interlayer

(Supplementary Table 1). These results suggest that DOC in the interlayer is less biodegradable than that at the surface or in deep soil.

Microbial diversity and community composition. The alpha diversity of bacteria was significantly lower in the interlayer than in the other two layers (Fig. 3a and Supplementary Fig. 6a–c). The composition of bacterial communities also differed significantly among the three layers (Fig. 3b). In contrast, the fungal alpha diversity did not differ (Fig. 3c and Supplementary Fig. 6d–f), and its community composition differed significantly among the three layers (Fig. 3d). The numbers of specific OTUs were lowest in the interlayer soil for both bacteria and fungi. The highest number of specific OTUs were at the surface for bacteria and in deep soil for fungi (Fig. 3e, g).

Among the bacterial phyla showing a relative abundance >0.5%, *Proteobacteria*, *Bacteroidetes*, and *Atribacteria* were significantly more abundant in the interlayer than in the other two layers. And the surface contained significantly more *Actinobacteria*, *Acidobacteria*, *Verrucomicrobia*, *Nitrosirae*, and *Planctomycetes* than the other two layers (Fig. 3f and Supplementary Table 2). Among the bacterial genera showing relative abundance >0.5%, *Pseudolabrys*, *Bradyrhizobium*, *Nitrosospira*, and *Natronoflexus* were significantly higher at the surface than the other two layers. Conversely, *Geobacter* was significantly higher in the deep soil than the other two layers. *Burkholderia*, *Variovorax*, *Duganella*, *Pseudomonas*, and *Mucilaginibacter* were highest, and *Dehalococcoides* was lowest at the interlayer (Fig. 4a and Supplementary Table 2).

The dominant functional groups of bacteria (>1%) did not differ among the three layers, except for groups of Replication and repair and Cell motility, both of which were significantly higher at the interlayer than the other two layers, and the group of Cell growth and death which was significantly lower at the interlayer than the other two layers (Supplementary Table 3).

Among fungal classes showing relative abundance >0.5%, Dothideomycetes was significantly more abundant in the interlayer and deep soil than at the surface. Conversely, Leotiomycetes and Sordariomycetes were more abundant at the surface than the other two layers, and Tremellomycetes, Pezizomycetes, and Microbotryomycetes were more abundant in the interlayer than in the surface and deep soil (Fig. 3h and Supplementary Table 4). Among the fungal genera showing relative abundance >0.5%, *Paraphaeosphaeria* was significantly more abundant in the deep soil than in the other two layers, while *Dioszegia*, *Filobasidium*, and *Phoma* were significantly more abundant in the interlayer than in the other two layers (Fig. 4b and Supplementary Table 4).

CO_2 emission and its response to warming. Under anoxic conditions, the CO_2 emission was significantly lower at the interlayer than at the surface and deep soil (Fig. 5a, b). 10 °C warming accelerated CO_2 emission of three layers, with a significant increment of 32.53 µg g^{-1} d^{-1} at the surface and 19.2 µg g^{-1} d^{-1} in the deep soil. The increment at the interlayer was 12.3 µg g^{-1} d^{-1} (Fig. 5a). The Q_{10} parameter of CO_2 emission was higher at the surface than the emission from the interlayer or deep soil (Fig. 5b).

Under oxic conditions, the CO_2 emission rate increased in all three layers than under anoxic conditions, with an increased proportion of 12.3% at the surface, 61.7% at the interlayer, and 35.7% in the deep soil (Fig. 5c, d). Warming further accelerated CO_2 emission by 108.7, 80.5, and 84.8% of the soil at the surface, interlayer, and deep, respectively. The Q_{10} value for soil CO_2 emission was higher under oxic conditions than under anoxic conditions (Fig. 5d).
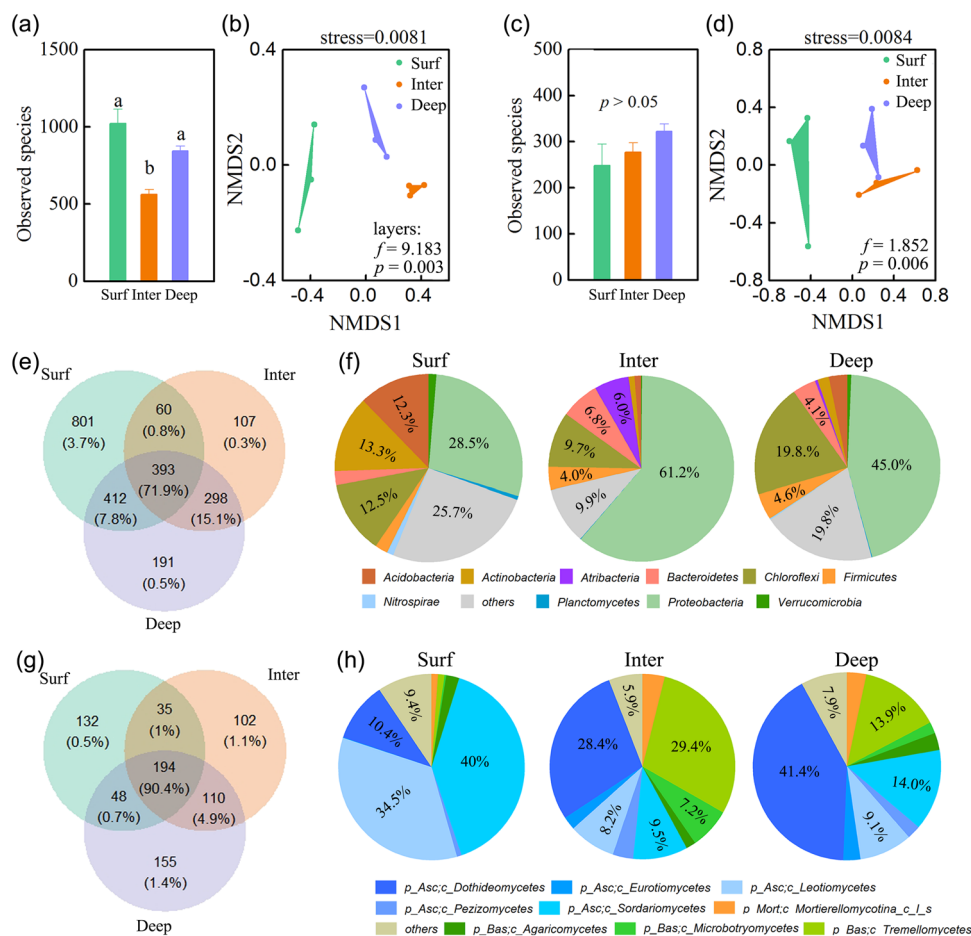
Fig. 3 Comparison of bacterial and fungal diversity and composition in the three water table-dependent soil layers. a, c Alpha diversity of bacteria and fungi, defined in terms of the numbers of species observed. **b, d** Nonmetric multidimensional scaling ordinations of community dissimilarities among three layers, based on Bray-Curtis dissimilarity (f and p represent differences of community composition among layers). **e, g** Overlap and differences in unweighted numbers of bacterial and fungal OTUs. **f, h** Relative abundances of bacterial phyla and fungal classes showing >0.5% abundance. Surf surface, Inter interlayer.

Soil variables response to warming. In all three layers, warming and oxygen significantly altered soil variables (Table 1). At the surface, nearly all these parameters increased under warming conditions, DOC, and NH_4^+-N also significantly increased under oxic conditions. H_2O-PHE, MBC, peroxidase activity, NO_3^--N and NH_4^+-N significantly increased under the combination of oxic and warming. Similar results were observed in the interlayer, except that the activity of phenolic oxidase significantly decreased under warming conditions. In deep soil, DOC and cellobiohydrolase significantly increased under warming conditions, and MBN, phenolic oxidase, peroxidase, and cellobiohydrolase significantly increased under oxic combined warming conditions. In addition, MBC significantly increased under warming, oxic, and their combined conditions.

Determinant of CO_2 emission at each layer. Pearson correlation was used to detect relationships between original properties and CO_2 emission of three layers of soil (Fig. 6). Regardless of the presence or absence of warming and the presence or absence of oxygen, the CO_2 emission rate correlated with Alkyl-C, the size of the fast carbon pool, MBC, MBN, bacterial diversity, H_2O-PHE and NO_3^--N (Fig. 6 and Supplementary Table 5). CO_2 emission rate also correlated with O-alkyl-C and NH_4^+-N under warming in the presence or absence of oxygen. In contrast, the CO_2

emission rate did not correlate with degradation indexes under any of the conditions tested.

The taxon of bacteria and fungi and functional groups of bacteria also correlated with CO_2 emission of three layers of soil. Under anoxic conditions, with or without warming, the CO_2 emission rate significantly correlated with the abundance of the bacterial phyla *Proteobacteria*, *Acidobacteria*, *Bacteroidetes*, *Verrucomicrobia*, *Nitrospirae*, and *Planctomycetes*, as well as the bacterial genera *Natronoflexus*, *Mucilaginibacter*, *Pseudomonas*, *Variovorax*, and *Clostridium*. Under oxic conditions, the CO_2 emission rate correlated with the bacterial phyla *Atribacteria* and bacterial genera *Clostridium* and *Dehalococcoides*. Under oxic-warming conditions, the CO_2 emission rate also correlated with the bacterial phyla *Proteobacteria*, *Bacteroidetes*, and *Verrucomicrobia*, as well as the bacterial genera *Pseudolabrys*, *Nitrosospira*, *Burkholderia*, *Mucilaginibacter*, *Pseudomonas*, *Variovorax*, and *Duganella* (Supplementary Table 6). The CO_2 emission only correlated with the bacterial functional group of Replication and repair under warming conditions, and groups of Cell motility and Cell growth and death under anoxic, warming, and oxic-warming conditions (Supplementary Table 7).

Under anoxic conditions, the CO_2 emission rate significantly correlated with the fungal class Tremellomycetes and Microbotryomycetes, as well as the fungal genera *Vishniacozyma*, *Vishniacozyma*, *Dioszegia*, and *Phoma*. Under warming conditions,
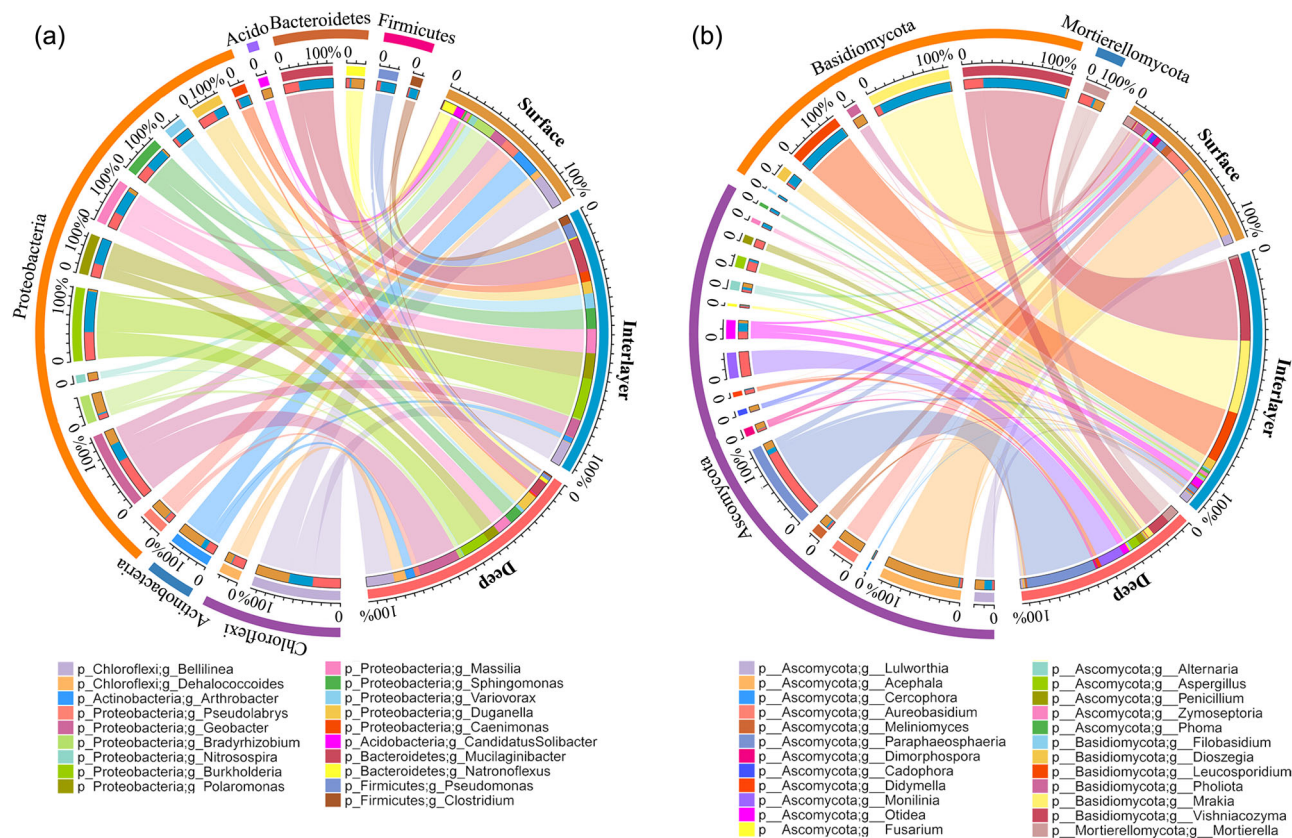
Fig. 4 Comparison of the bacterial and fungal genera abundance in the three water table-dependent soil layers. a bacteria; **b** fungi (showing relative abundance >0.5%); Acido: Acidobacteri (data and difference of each genus among three layers were shown in Supplementary Tables 2 and 4).

the CO_2 emission rate significantly correlated with the fungal genera *Dioszegia, Phoma, Zymoseptoria*, and *Filobasidium*. Under oxic combined warming conditions, the CO_2 emission rate significantly correlated with the fungal class Sordariomycetes and Pezizomycetes, as well as the fungal genera *Lulworthia, Otidea, Dioszegia*, and *Phoma* (Supplementary Table 8).

CO_2 emission from each soil layer seemed to be regulated by different soil variables (Table 2). At the surface soil, CO_2 emission mainly correlated with H_2O-PHE, DOC, MBC, MBN, peroxidase, β−1-4-glucosidase, NO_3^--N, and NH_4^+-N. At the interlayer, CO_2 emission mainly correlated with DOC, MBC, MBN, phenolic oxidase, peroxidase, β−1-4-glucosidase, NO_3^--N, and NH_4^+-N. CO_2 emission from deep soil correlated with MBC and enzyme activities. After grouping the soil variables into three groups through principal component analysis (Supplementary Table 9), the first principal component explaining most of the variation in emission from each soil layer was entered into the structural equation model (Fig. 7).

The resulting model explained 88% of the variation in CO_2 emission at the surface. Soil carbon quality and decomposers had a direct positive effect on CO_2 emission, while carbon quality also indirectly affected CO_2 emission through its negative correlation with decomposers and its positive correlation with N nutrients. Soil N nutrients indirectly affected CO_2 emission through its positive correlation with decomposers. Warming and oxygen indirectly affected CO_2 emission through their positive correlation with soil carbon quality. Taken together, carbon quality emerged as the most influential predictor of CO_2 emission at the surface, based on standardized effect coefficients (Fig. 7a).

The structural equation model explained 94% of the variation in CO_2 emission in the interlayer, where decomposers and N nutrients affected the emission rate directly as well as indirectly through their negative correlation with each other. Temperature indirectly affected

CO_2 emission through its positive correlation with decomposers, and oxygen indirectly affected CO_2 emission through its positive correlations with decomposers and N nutrients. In contrast to the results at the surface, N nutrients emerged as the most influential predictor of CO_2 emission from the interlayer (Fig. 7b).

The structural equation model explained 79% of the variation in CO_2 emission in deep soil, in which decomposers were the major determinant. Neither carbon quality nor N nutrients correlated significantly with CO_2 emission, whereas temperature and oxygen affected CO_2 emission indirectly through their positive correlation with decomposers. Thus, decomposers emerged as the most influential predictors of CO_2 emission from deep soil (Fig. 7c).

Discussion

We measured mean CO_2 emission rates from 24.97 ± 0.21 to $43.87 \pm 3.86\ \mu g\ g^{-1}\ d^{-1}$ across the three water table-dependent soil layers during 154-day incubation, which falls at the low end of the range reported for tropical peatlands (193–$1864.8\ \mu g\ g^{-1}\ d^{-1}$)[37,38]. Higher emission from tropical peatlands has been attributed to higher carbon quality, greater nutrient availability, and lower proportions of recalcitrant carbon[38]. Consistent with this, the C/N ratio, which can indicate carbon quality[21], ranges from 20.3 to 47 on tropical peatlands[39–41], much higher than the range of 15.09–19.45 in our study.

Our mean CO_2 emission rates are at the high end of the range reported for boreal peatlands[42,43]. This suggests that carbon on boreal peatlands is less vulnerable than carbon on Zoige peatlands, which may reflect differences in vegetation, the main source and predictor of carbon liability. The dominant vegetation on Zoige peatlands is herbaceous, featuring graminoids and sedges, whereas dwarf shrubs and moss predominate on peatlands at higher
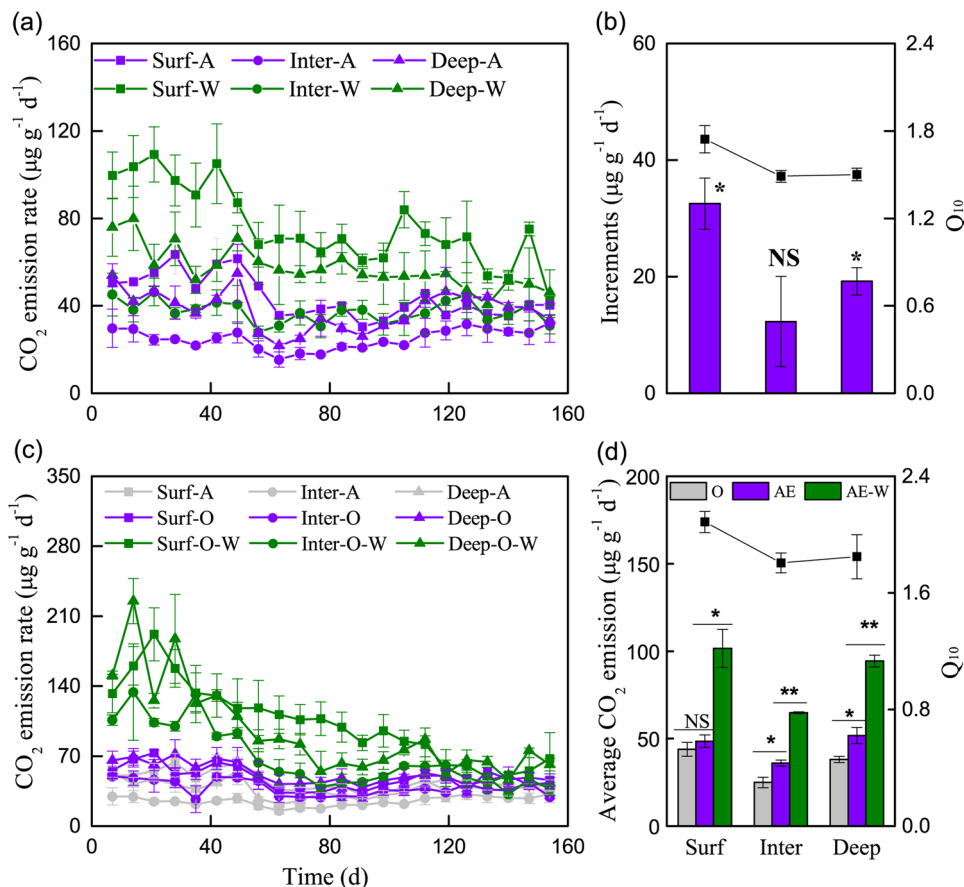
Fig. 5 Comparison of CO$_2$ emission rate from the three water table-dependent soil layers under different oxygen and temperature conditions.
a, **c** Emission during 154 days of incubation under anoxic and oxic conditions. **b** Increases in CO$_2$ emission as a result of warming and the Q$_{10}$ of CO$_2$ emission under anoxic conditions. Absolute increases are shown on the left vertical axis, while Q$_{10}$ values are plotted on the right vertical axis. Increases were assessed for significance using the t-test. **d** Differences in emission depending on the oxygen conditions and temperature, and the Q$_{10}$ of CO$_2$ emission under oxic conditions. Absolute rates are plotted on the left vertical axis and Q$_{10}$ values on the right vertical axis. (Paired t-test. *$p < 0.05$, **$p < 0.01$; NS no significant difference). Surf surface, Inter interlayer, A anoxic conditions, O oxic conditions, W warming.

Table 1 Significance of variation in variables across the three water table-dependent soil layers during incubation.

Variables	Surface			Interlayer			Deep		
	T	O$_2$	O$_2$ × T	T	O$_2$	O$_2$ × T	T	O$_2$	O$_2$ × T
DOC	**0.008**↑	**0.029**↑	0.082	0.159	0.063	**0.031**↑	**0.049**↑	0.124	0.116
H$_2$O-PHE	**0.004**↑	0.328	**0.004**↑	0.069	0.487	0.973	0.624	0.536	0.127
MBC	**0.024**↑	0.757	**0.010**↑	**0.019**↑	0.084	**0.005**↑	**0.001**↑	**0.005**↑	**0.000**↑
MBN	**0.046**↑	0.858	0.069	**0.011**↑	0.230	**0.005**↑	0.573	0.053	**0.031**↑
Phe-ase	0.296	0.805	0.376	**0.017**↓	0.782	0.255	0.578	0.075	**0.001**↓
PerO-ase	**0.014**↑	0.574	**0.044**↑	**0.000**↑	**0.040**↑	**0.006**↑	0.091	0.165	**0.012**↑
Glu-ase	0.361	0.890	0.140	**0.003**↑	0.239	**0.001**↑	0.189	0.628	0.074
Cell-ase	0.111	0.195	0.105	0.218	0.298	0.441	**0.001**↑	0.509	**0.004**↑
NO$_3^-$-N	**0.015**↑	0.076	**0.000**↑	0.430	**0.015**↑	**0.001**↑	0.106	0.687	0.079
NH$_4^+$-N	**0.009**↑	**0.004**↑	**0.005**↑	**0.012**↑	**0.013**↑	**0.008**↑	0.578	0.749	0.194

Significance values refer to a t-test between control and treatments.
Bold denotes significant variation; ↑ and ↓ denote significant increases or decreases relative to the control.
T warming, O_2 oxic conditions, O_2 × T oxic conditions with warming, *DOC* dissolved organic carbon, *H$_2$O-PHE* water-soluble phenolics, *MBC* microbial biomass carbon, *MBN* microbial biomass nitrogen, *Phe-ase* phenolic oxidase, *PerO-ase* peroxidase, *Glu-ase* β−1-4-glucosidase, *Cell-ase* cellobiohydrolase.

latitudes[44]. The higher carbon quality of herbaceous litter in comparison to moss and shrubs litter could then result in a higher CO$_2$ emission rate on the Zoige Plateau. Another contributor to the greater CO$_2$ emission from the Zoige Plateau is minerotrophic peat, abundant in nutrients from rivers[45]; boreal peatlands, in contrast, is ombrotrophic with poor nutrients[46]. In addition, the higher incubation temperature also is a reason of higher CO$_2$ emission rate on the Zoige Plateau.

Our study illuminates a relatively stable interlayer and relatively vulnerable surface and deep soil in terms of CO$_2$ emission on the Tibetan Plateau. In our laboratory incubation, CO$_2$ emission was greater from the surface than from the other two
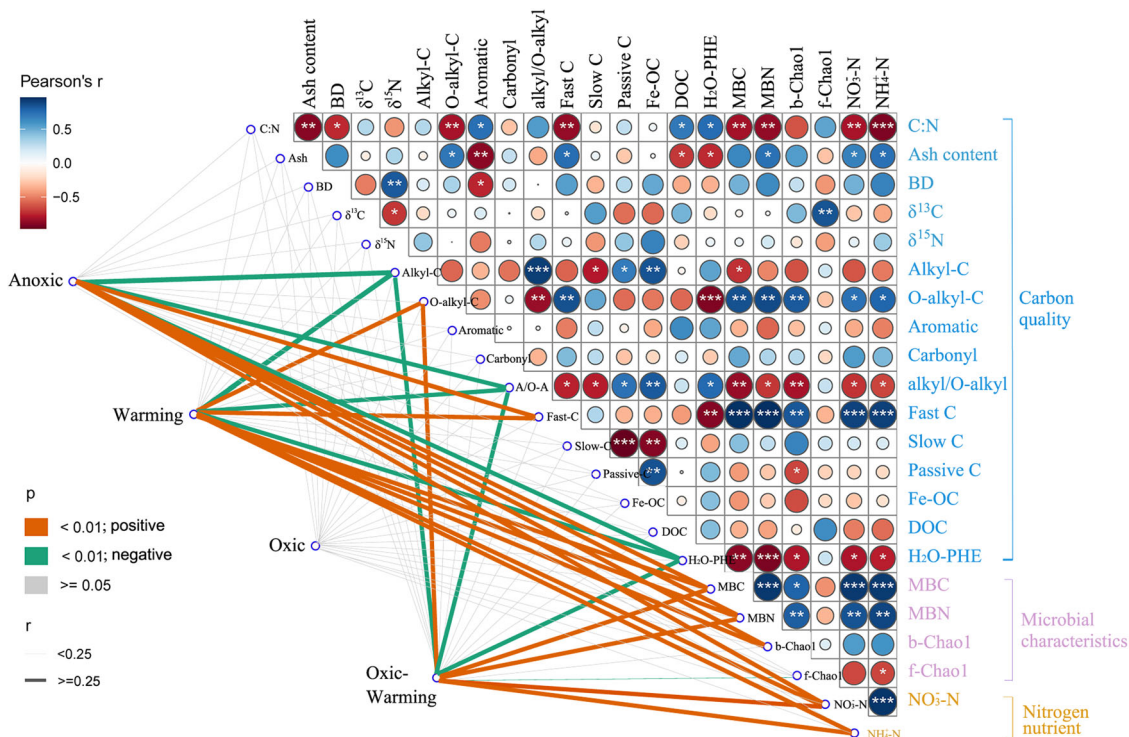
Fig. 6 Correlations between CO$_2$ emission rate and soil properties under different oxygen and temperature conditions. Line width reflects the Pearson correlation coefficient, while line color reflects the nature of the correlation (positive or negative) and the associated p value. In the matrix of pairwise comparisons, Pearson correlation coefficients are indicated using a color gradient. ***$p < 0.001$, **$p < 0.01$, *$p < 0.05$. BD bulk density, A/O-A ratio of alkyl-C to O-alkyl-C, DOC dissolved organic carbon, H$_2$O-PHE water-soluble phenolics, Fe-OC, Fe-bound organic carbon, MBC microbial biomass carbon, MBN microbial biomass nitrogen, b-Chao1 Chao1 richness of bacteria, f-Chao1 Chao1 richness of fungi.

Table 2 Correlations between soil CO$_2$ emission and soil variables at each layer ($n = 12$).

Soil layer		Carbon quality		Decomposers						Nitrogen nutrients	
		DOC	H$_2$O-PHE	MBC	MBN	Phe-ase	PerO-ase	Glu-ase	Cell-ase	NO$_3^-$-N	NH$_4^+$-N
Surface	r	**0.647***	**0.814****	**0.883*****	**0.638***	0.560	**0.741****	**0.741****	0.541	**0.619***	**0.822****
	p	**0.023**	**0.001**	**0.000**	**0.026**	0.058	**0.006**	**0.006**	0.069	**0.032**	**0.001**
Interlayer	r	**0.634***	0.035	**0.722****	**0.774****	**0.603***	**0.914*****	**0.751****	0.279	**0.697***	**0.892*****
	p	**0.027**	0.914	**0.008**	**0.003**	**0.038**	**0.000**	**0.005**	0.379	**0.012**	**0.000**
Deep	r	0.517	−0.526	**0.695***	0.474	**0.699***	**0.691***	**0.618***	**0.791****	0.564	0.391
	p	0.085	0.079	**0.012**	0.120	**0.011**	**0.013**	**0.032**	**0.002**	0.056	0.209

Bold denotes significant correlation. ***$p < 0.001$, **$p < 0.01$, *$p < 0.05$.
DOC dissolved organic carbon, *H$_2$O-PHE* water-soluble phenolics, *MBC* microbial biomass carbon, *MBN* microbial biomass nitrogen, *Phe-ase* phenolic oxidase, *PerO-ase* peroxidase, *Glu-ase* β—1-4-glucosidase, *Cell-ase* cellobiohydrolase.

layers. This may reflect the greater carbon quality and microbial activity at the surface[12,14]. Plant roots and litter supply abundant labile carbon to surface soil[47], increasing the content of O-alkyl-C and N nutrient and enhancing microbial activity[48]. Greater CO$_2$ emission rate at the surface soil may also reflect the predominance of aerobic microbes, such as the bacteria of *Bradyrhizobium*, *Nitrosospira*, and *Natronoflexus*[49] and fungi of *Lulworthia* and *Acephala*[50]. Lower CO$_2$ emission rate at deeper two layers mainly because of the exhaustion of labile nutrients for microbes during long-term slow decay[51]. This result further reflects that the carbon at the deeper two layers was more degraded, with a higher C/N ratio and δ^{13}C, low bulk density. Higher δ^{15}N at surface soil may result from the increasing human activity and nitrogen deposition[52].

Surprisingly, our study found that the CO$_2$ emission rate was lowest in the interlayer, rather than in deep soil. Such phenomena could attribute to the highest proportion of recalcitrant/passive carbon at the interlayer. Long-term water table fluctuation exposes interlayer soil to secondary oxic decomposition, during which labile carbon and nutrients had been consumed and recalcitrant carbon was accumulated[21,53]. Accompanied by a high content of recalcitrant carbons, the bacterial diversity and number of specific OTU were also lowest at the interlayer, partially explaining the lowest CO$_2$ emission at interlayer[25,47,54]. This result suggests that the interlayer in drained peatlands is stable in CO$_2$ emission.

Compared with the interlayer, higher CO$_2$ emission in the deep soil may be because of the preferential flow of nutrients from the surface[17,55]. The accumulation of nutrients in anoxic deep soil increases labile carbon content and CO$_2$ emission rate[35]. In addition, the deep soil in our study contained highly diverse fungal communities and high numbers of specific OTU. These
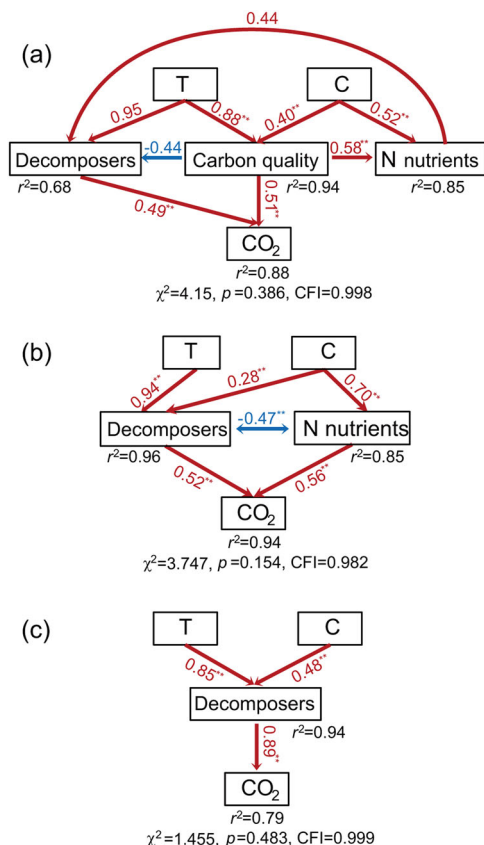
Fig. 7 Structural equation modeling to describe the effects of factors on the CO_2 emission rate of three layers soil. a surface, **b** interlayer, **c** deep soil. Arrows indicate the hypothesized direction of causation. Red indicates a positive relationship; blue indicates a negative one. Arrows are labeled with standardized path coefficients (*$p < 0.05$, **$p < 0.01$), and the proportion of variance explained (r^2) is indicated below the variables. At the bottom of the models are goodness-of-fit statistics. N nutrients nitrogen nutrients, T temperature, C incubation conditions.

factors also contribute to the higher CO_2 emission, given that fungi prefer to metabolize complex carbons to obtain energy[56].

Our study further illuminates that the three layers responded differently to warming. In specific, warming greatly increased CO_2 emission at the surface soil, presumably because of its greater abundance of microbes, which are reported to be temperature responsive[28]. Warming also greatly increased CO_2 emission in deep soil, because of its higher content of inherently biochemical recalcitrant carbon, such as aromatic compounds, which are more responsive to warming than physically protected carbons[57,58]. Consistent with these explanations, the concentration of DOC, which could be accessed by microbes directly[12], also greatly increased by warming at the surface and deep soil, supporting the enhancement of CO_2 emission. At deep soil, the increased DOC even could serve as exogenous carbon inputs to cause positive priming[10], accelerating CO_2 emission[17,18]. Together with other studies on alpine peatlands, which also reported that deep soil was temperature sensitive[15,35], our results suggest that deep soil carbon is recalcitrant, but still vulnerable to warming.

At the interlayer, warming increased microbial activity and, thereby, CO_2 emission, whereas to a smaller extent than in the other two soil layers. This may be attributed to the fact that the interlayer contained the highest proportion of mineral-protected carbon, here measured as Fe-OC, and this form of carbon is reported as less sensitive to warming than other forms, such as

biochemically recalcitrant carbons[57,58]. We postulate that following long-term secondary oxic decay, the severely degraded carbon in the interlayer is not only recalcitrant but also insensitive to warming. In this case, previous depth-dependent studies may have overestimated the vulnerability[10,59] and warming sensitivity[10,19,35] of carbon in the deeper soil.

Exposing the three layers of soil to oxic conditions hugely increased CO_2 emission, which was further greatly increased under oxic combined warming conditions. Sufficient oxygen activates aerobic microbes such as the bacteria *Rhizobiales*, *Nitrospirales*, and *Caulobacterales*, and fungi of *Helotiales* and *Pleosporales*[60]. These aerobic microbes, especially the fungi, secrete a wide range of enzymes to break down recalcitrant compounds to meet their demands for energy and nutrients[56], and enhancing the CO_2 emission. Indeed, we found that the activity of peroxidase and $\beta-1-$ 4-glucosidase in the interlayer and the activity of peroxidase and phenol oxidase in the deep soil substantially increased when under oxic conditions. These results suggest that microbial and enzyme activity are severely constrained under anoxic conditions, which then maintain the stability of peatlands carbon stock.

At last, our study presents direct evidence of different determinants mediating CO_2 emission in each soil layer. As shown by SEM, carbon quality was the primary determinant of CO_2 emission from the surface soil. Soil carbon can be divided into three pools[61,62] according to their turnover time, and the fast pool is small and can be depleted in a few months[26,63]. Thus, the remained slow and passive carbon pool, which size is large and with a turnover time of thousands to centuries years[64], may be the direct regulator of CO_2 emission from the surface soil. During incubation in the present study, the contribution of the fast carbon pool to total respired CO_2 was reduced, and the contribution from the slow and passive carbon pool progressively increased (Supplementary Fig. 7). Thus, we postulate that carbon quality, especially the slow and passive carbon pools, will determine CO_2 loss from drained peatlands in the long term. Previous studies came to divergent conclusions about whether the major determinants of CO_2 emission from surface soil of drained peatlands were carbon quality, nutrient content[13], or microbial activity[65]. Their divergent findings may reflect a failure to account for the environmental gradient caused by water table fluctuation.

In contrast to the situation at the surface, we found that decomposers became the primary determinant of CO_2 emission in deep soil. The study reports that genes coding for enzymes are greatly higher in recalcitrant carbon-rich soils than in other soils[66], because microbes should strongly upregulate enzyme secretion to decompose recalcitrant carbon to obtain energy and nutrients[36,66]. And warming could further upregulate such genes in bacteria and fungi[15], which help explain the enhanced CO_2 emission from deep soil in our study. In this way, our study indicates that decomposers are the primary drivers of CO_2 emission from deep soil, especially fungi which has enzymatic potential to decompose recalcitrant carbon[36,61].

Similarly, decomposers were a major determinant of CO_2 emission from the interlayer, because of its rich recalcitrant carbon and microbes need to produce a wide range enzymes to obtain energy and nutrients[36,66]. Interestingly, our results showed that the N nutrient, with the highest standardized path coefficients, was the primary factor mediating the CO_2 emission at the interlayer. The content of NO_3^--N and NH_4^+-N increased under oxic or warming conditions and correlated with MBC and CO_2 emission rates. This result suggests the sensitivity of microbial metabolism to N nutrients[67], in part because nitrogen is required for microbes in order to produce extracellular enzymes[17,68].

While our study provides experimental evidence that the carbon stability is distinct among water table-dependent three layers of drained peatlands. At the same time, our results should be

interpreted with caution in light of several limitations: first, our incubation experiment did not consider the influence of vegetation, leading to uncertainty in explaining the determinant of CO_2 release at each layer on a large scale. Second, serving the average water table as the base to divide the surface and interlayer, may lead to inaccuracy in evaluating the magnitude and determinant of CO_2 release of each layer when in field, because such surface soil also could be waterlogged after heavy rain. In situ experiments, including the influence of vegetation and reasonable stratification of the vertical profile, are needed to clarify the carbon stability of drained peatlands.

Despite these limitations, our study suggests that the carbon stability of drained peatlands differs across their water table-dependent soil layers, because of the differences in soil carbon quality as well as microbial diversity and activity. We find that oxic surface and anoxic deep soil are vulnerable and sensitive to warming in CO_2 emission, for the highest MBC at the surface soil and chemically recalcitrant carbon in the deep soil. The major determinant of CO_2 emission at these two layers are carbon quality and decomposers, respectively. However, experiencing periodic oxic decay, the CO_2 emission at the interlayer is stable and less sensitive to warming than the other two layers, and N nutrients become its major driver of CO_2 emission.

Our findings suggest that the CO_2 loss from drained peatlands in previous depth-dependent studies may be unfaithful because they omit the interlayer along the soil profile which is caused by the heterogeneity of environments like oxygen and hydrology. Future research should include the environmental gradient along the soil profile. Our findings also highlight the need to incorporate N nutrient into Earth System Models for precisely predicting carbon loss from drained peatlands under climate change.

Methods

Site description and sampling. Our study site was located at Ruokeba on the Zoige Plateau, which lies in the northeastern part of the Qinghai-Tibet Plateau (33°03′58″N, 102°34′39″E, avg. 3470 m a.s.l; Supplementary Fig. 2a). Annual mean temperature on the Zoige plateau is 3.3 °C and annual mean precipitation is 705 mm. Peatlands on the Zoige Plateau are minerotrophic fens where peat has been accumulating since the early Holocene due to the low temperature and abundant precipitation. Currently peat on the Zoige Plateau covers 4605 km^2 to a mean depth of 1.39 m (range, 0.2 to 6.0 m)[69]. Dominant vegetation at Ruokeba peatlands is *Equisetum ramosissimun, Scirpus triqueter*, and *Blysmus sinocompressus*.

The peatlands on Zoige plateau, including Ruokeba, experienced severe drainage in the 1970s[70]. Currently, the ditch has a depth of 30–50 cm and acts as the main channel for transporting water and DOC from peatlands to lower regions (Supplementary Fig. 2b). Based on measurements since 2015 using a 1-m grid, the water table on Ruokeba peatland averages −25 cm, ranging from −4 to −67 cm below the soil surface (Supplementary Fig. 2c). As a result, we divided the soil layers for the present study as follows: surface, above a depth of 25 cm; deep, deeper than a depth of 75 cm; and interlayer, from a depth of 25 cm to a depth of 75 cm.

Three plots with similar water table fluctuation range at Ruokeba were randomly selected, and five soil columns (105 cm) were collected at each plot using a vibracore with a diameter of 8 cm. For each soil layer, the soil from the five columns at each plot was combined into a single sample. Each sample was transported to the laboratory in an ice cooler and divided into two fractions, one of which was subjected to microbial analysis, while the other was subjected to lab incubation and soil properties analyses.

Lab incubation. After removing large roots, 80 g of homogenized soil of each layer was put into a 500-ml glass jar, which was then sealed with a rubber stopper with two openings for sampling and gas exchange. For 154 days, jars were incubated in the dark under both anoxic conditions in which the headspace was flushed with N_2 (99.9%) and oxic conditions in which the headspace was flushed with CO_2-free air (containing O_2: 21%; N_2: 79%; 99.9%), and at two temperatures: 8 °C as control (the average temperature during the growing season on the Zoige Plateau) and 18 °C as warming (10 °C warming to get a reliable Q_{10} of CO_2 emission). The flow rate and timing of gas flush was set through a continuous monitor[71]. The four treatments were anoxic (control), warming, oxic, oxic combined warming, and these experiments involved 36 samples: 3 soil layers × 2 conditions × 2 temperatures × 3 replicates.

During the incubation, headspace gas was sampled weekly. At 12 h before each sampling, the headspace was evacuated and flushed with N_2 or CO_2-free air again to remove the accumulated CO_2. CO_2 concentration in the headspace gas was measured using gas chromatography (Agilent 7890 A, Wilmington, DC, USA) as

described in ref. [71]. The Q_{10} parameter was roughly estimated using the ratio of CO_2 emission at 18 to 8 °C.

Soil carbon degradation indexes. Indexes indicating soil carbon degradation degree were C/N ratio, ash content, bulk density (BD), $\delta^{13}C$, and $\delta^{15}N$[72]. The C/N ratio was calculated as the ratio of %C to %N, both of which were determined using an elemental analyzer (Elementar, Langenselbold, Germany)[73]. Ash content was measured using thermogravimetry[72], and BD was measured using a bulk soil sampler[74]. Stable isotopes of $\delta^{13}C$ and $\delta^{15}N$ in soil were analyzed using an isotope ratio mass spectrometer (Thermo Scientific, Waltham, MA, USA) and the Vienna Pee Dee Belemnite standard.

Soil chemical components. Chemical components in soil carbon were quantified using solid-state ^{13}C CPMAS NMR. Magic-angle spinning experiments were conducted on an Avance III 400WB solid-state spectrometer (Bruker, Berlin, Germany) using 3.2-mm double-resonance probes spinning at 15 kHz. Spectra were collected at the ^{13}C Larmor frequency of 100.6 MHz. ^{13}C cross-polarization contact time was 2 ms, and ^1H decoupling power was 104.2 kHz. ^{13}C signals were referenced to the methylene signal of adamantane at 38.5 ppm, and the spectra were analyzed in the following chemical shift regions using MestReNova 9.0 (MESTRELAB Research, Santiago de Compostela, Galicia, Spain): alkyl-C, 0 to 50 ppm; O-alkyl-C, 50 to 110 ppm; aromatic-C, 110 to 165 ppm; and carbonyl-C, 165–220 ppm[75]. The concentration of Fe-OC was measured using the citrate-bicarbonate-dithionite method[76].

Levels of labile organic carbon present as H_2O-PHE and DOC. The concentration of H_2O-PHE in soil was estimated using the Folin-Ciocalteu method, with p-hydroxybenzoic acid as the standard. Incubated fresh soil (5 g) and deionized water (25 ml) were shaken at a frequency of 200 rpm for 20 h, filtered through a 0.45-μm filter, and diluted 1:5. An aliquot (1 ml) was mixed with 2 ml Na_2CO_3-$NaHCO_3$ buffer (pH 10), 1 ml Folin-Ciocalteu reagent, and 1 ml Na_2CO_3 (0.4 mol l^{-1}), then incubated for 15 min at 37 °C in the dark. Absorbance at 750 nm was measured using a spectrophotometer (Thermo Spectronic 200, Waltham, MA, USA). Standard phenolic absorbance was also measured with the same procedure. The concentration of H_2O-PHE, expressed as mg g^{-1} soil, was calculated as described in ref. [77]. Levels of DOC was measured using a continuous flow analyzer (San++, SKALAR, Delft, Netherlands).

Soil carbon pool model. SOC could be conceptually grouped into three pools: *fast pool* with a turnover time of a few days to a few months, *slow pool* with a turnover time of about a few years, and *passive pool* with a turnover time of a few years to thousands of years[78]. Carbon in passive pools also belongs to recalcitrant carbons whose turnover time is about centuries to millennia years[79]. The size of different carbon pools of each layer was estimated using the three-pool model[63], which integrates data from three replicates incubated under anoxic conditions into Eq. (1):

$$R(t) = k_1 f_1 C_{tot} e^{-k1t} + k_2 f_2 C_{tot} e^{-k2t} + k_3(1 - f_1 - f_2) C_{tot} e^{-k3t} \quad (1)$$

where R(t) is the CO_2 emission rate at time t (mg C g^{-1} d^{-1}); C_{tot} is the initial soil carbon content; f_1 and f_2 refer to the fast pool fraction and slow pool fraction, respectively; and k_1, k_2, and k_3 are the decay rates for fast, slow and passive carbon pools, respectively. C_{tot} and R(t) were measured experimentally, while the other parameters were estimated using a Markov Chain Monte Carlo approach[80]. The prior parameter range of Markov Chain Monte Carlo analysis was set in Supplementary Table 10, which was as wide as possible to cover the possibility of three-layer soils.

Soil microbial properties. Microbial biomass carbon (MBC), microbial biomass nitrogen (MBN), microbial diversity, and community composition were determined. MBC and MBN were measured using chloroform fumigation.

Microbial diversity and community composition were determined using high-throughput sequencing of soil DNA, which was extracted using the PowerSoil Kit (MoBio Laboratories, Carlsbad, CA, USA) following the manufacturer's instructions. The V4 region of the bacterial 16 S rRNA gene and the ITS1 region of fungi were amplified using PCR to characterize the bacterial and fungal communities, respectively. The primers of V4 region was 515 F (5′- GTGCCAG CMGCCGCGGTAA-3′) and 806 R (5′-GGACTACHVGGGTWTCTAAT-3′)[81], and ITS1 region was amplified with primers ITS1f (5′-CTTGGTCATTTAGAG GAAGTAA-3′)[82] and ITS2 (5′GCTGCGTTCTTCATCGATGC-3′)[83]. Sequencing was performed using the 2 × 300 paired-end Miseq PE300 platform (Illumina, USA) at Allwegene Tech Beijing (Beijing, China).

QIIME was used to filter raw sequences to obtain higher-quality clean tags (length, 250–500 bp, average base quality score >25). After removing chimeric sequences using the UCHIME algorithm, sequences with ≥97% similarity were assigned to the same operational taxonomic unit (OTU) based on the SILVA database (bacteria) and UNITE database (fungi). The OTU abundances were normalized using a standard sequence number corresponding to the sample with the fewest sequences (14,130 for bacteria and 22,169 for fungi). The normalized OTU was used in the downstream analysis of bacteria and fungi. The bacterial and fungal sequences of three layers of soil were retrieved from published 16 S and ITS sequences (deposited in the NCBI Sequence Read Archive (SRA) database with accession number SRP211776)[60].

Soil enzyme activity. Four enzymes activity were measured as described in refs. [84,85] in a 96-well plate assay. Phenol oxidase and peroxidase were assayed spectrophotometrically, while $\beta-1,4$-glucosidase and cellobiohydrolase were assayed fluorimetrically.

Soil nitrogen levels. Levels of NO_3^--N and NH_4^+-N were measured using a continuous flow analyzer (San++, SKALAR, Delft, Netherlands).

Data analysis. During data analysis, carbon degradation indexes, carbon chemical components (alkyl, O-alkyl, aromatic, carboxylic), Fe-bound organic carbon (Fe-OC), and size of carbon pools[78,86,87] were used to describe soil carbon quality. Microbial properties and enzyme activities were used to describe soil decomposers. Nitrogen levels of NO^-_3-N and NH_4^+-N were listed as N nutrients. In addition, soil labile carbon levels, MBC, MBN, enzyme activity, NO_3^--N, and NH_4^+-N varied during incubation. Thus, these indexes were listed as soil variables and were measured to identify determinants of CO_2 release from each layer (Supplementary Fig. 1).

The diversity of bacteria and fungi were assessed using the *vegan* package (version 2.4-5) in R[88]. The composition of bacterial and fungal communities were assessed using ordination by nonmetric multidimensional scaling with the "metaMDS" function in *vegan*[89], and their difference among layers were assessed using permutational multivariate analysis of variance (PERMANOVA) with 999 permutations and an "ADONIS" function in *vegan*. Bacterial OTU were also assigned to a different functional group based on Tax4Fun package[90].

Before statistical analyses, data were confirmed to be normally distributed (Kolmogorov–Smirnov test); if not, they were log-transformed. The log-transformed indexes included DOC and bacterial diversity. All statistical analyses were performed using SPSS 20.0 for Windows (IBM, Chicago, IL, USA) with a significance definition of $p < 0.05$. Results were depicted graphically using Origin 8.0 (OriginLab, Northampton, MA, USA).

Differences in soil carbon quality, bacterial/fungal diversity, the relative abundance of each taxon of bacteria and fungi, bacterial functional groups, and CO_2 emission among the three layers were assessed for significance using one-way analysis of variance (ANOVA) with the Tukey HSD test. Differences in CO_2 emission between control and treatments were assessed using the paired t-test. The potential relationships between soil carbon quality/microbial properties of the original soil and CO_2 emission were accessed together of three layers of soil using Pearson correlation analysis. Pearson correlation analysis was also used to access the relationships between soil variables and CO_2 emission separately for each layer.

Piecewise structural equation model was conducted to identify determinants of CO_2 emission in each layer under different temperatures and incubation conditions. In this modeling, treatment was the exogenous variable, while soil variables were the endogenous variables. The modeling was carried out using the *semPlot* package in R.

The primary structural equation model was developed based on prior knowledge of regulators of CO_2 emission (Supplementary Fig. 3). Paths were drawn from temperature (T) and incubation conditions (C) to all endogenous variables, then to CO_2. This model was used in linear mixed-effect models. The least significant paths were removed stepwise from the model until none of the remaining parameters was associated with $p > 0.1$.

To simplify the structural equation model, soil endogenous variables were grouped into *carbon quality*, comprising H_2O-PHE and DOC; *decomposers*, comprising MBC, MBN, phenolic oxidase, peroxidase, $\beta-1,4$-glucosidase and cellobiohydrolase; and *N nutrients*, comprising NO_3^--N and NH_4^+-N. Within each of these three groups, principal component analysis was conducted using only those variables that correlated significantly with CO_2 emission. The first component, which could explain more than 60% of the total variation (Supplementary Table 9), was introduced as a new variable in the structural equation model[36].

Reporting summary. Further information on research design is available in the Nature Portfolio Reporting Summary linked to this article.

Data availability

The microbial data were available in the NCBI Sequence Read Archive (SRA) database (SRP211776). The remaining data supporting the findings of this study were deposited on figshare (https://doi.org/10.6084/m9.figshare.21580938.v1).

References

1. Yu, Z., Loisel, J., Brosseau, D. P., Beilman, D. W. & Hunt, S. J. Global peatland dynamics since the Last Glacial Maximum. *Geophys. Res. Lett.* **37**, L13402 (2010).
2. Joosten, H., Tapio-BiströmM, L. & Susanna, T. Peatlands: guidance for climate change mitigation through conservation, rehabilitation and sustainable use. Food and Agriculture Organization of the United Nations and Wetlands International. *FAO* (2012).
3. IUCN. Issues brief: peatlands and climate change. www.icun.org (2017).
4. Joosten, H. *Peatlands, Climate Change Mitigation and Biodiversity Conservation. An Issue Brief on the Importance of Peatlands for Carbon and Biodiversity Conservation and the Role of Drained Peatlands as Greenhouse Gas Emission Hotspots* (Nordic Council of Ministers, 2015).
5. Moore, T. R. & Knowles, R. The influence of water table levels on methane and carbon dioxide emissions from peatland soils. *Can. J. Soil Sci.* **69**, 33–38 (1989).
6. Tfaily, M. M. et al. Organic matter transformation in the peat column at Marcell Experimental Forest: humification and vertical stratification. *J. Geophys. Res. Biogeosci.* **119**, 661–675 (2014).
7. Clymo, R. S. & Bryant, C. L. Diffusion and mass flow of dissolved carbon dioxide, methane, and dissolved organic carbon in a 7-m deep raised peat bog. *Geochim. Cosmochim. Acta* **72**, 2048–2066 (2008).
8. Clymo, R. S. The limits to peat bog growth. *Philos. Trans. R. Soc. B* **303**, 605–654 (1984).
9. Qin, S. et al. Temperature sensitivity of SOM decomposition governed by aggregate protection and microbial communities. *Sci. Adv.* **5**, eaau1218. 1211–1219 (2019).
10. Dorrepaal, E. et al. Carbon respiration from subsurface peat accelerated by climate warming in the subarctic. *Nature* **460**, 616–619 (2009).
11. Luo, Z. K., Wang, G. C. & Wang, E. L. Global subsoil organic carbon turnover times dominantly controlled by soil properties rather than climate. *Nat. Commun.* **10**, 3688 (2019).
12. Wilson, R. M. et al. Stability of peatland carbon to rising temperatures. *Nat. Commun.* **7**, 13723 (2016).
13. Sihi, D., Inglett, P. W. & Inglett, K. S. Carbon quality and nutrient status drive the temperature sensitivity of organic matter decomposition in subtropical peat soils. *Biogeochemistry* **131**, 103–119 (2016).
14. Wang, Q., Liu, S. & Tian, P. Carbon quality and soil microbial property control the latitudinal pattern in temperature sensitivity of soil microbial respiration across Chinese forest ecosystems. *Glob. Chang. Biol.* **24**, 2841–2849 (2018).
15. Cheng, L. et al. Warming enhances old organic carbon decomposition through altering functional microbial communities. *ISME J.* **11**, 1825–1835 (2017).
16. Luan, J., Wu, J., Liu, S., Roulet, N. & Wang, M. Soil nitrogen determines greenhouse gas emissions from northern peatlands under concurrent warming and vegetation shifting. *Commun. Biol.* **2**, 132 (2019).
17. Meyer, N. et al. Nitrogen and phosphorus supply controls soil organic carbon mineralization in tropical topsoil and subsoil. *Soil Biol. Biochem.* **119**, 152–161 (2018).
18. Fontaine, S. et al. Stability of organic carbon in deep soil layers controlled by fresh carbon supply. *Nature* **450**, 277–280 (2007).
19. Moni, C. et al. Temperature response of soil organic matter mineralisation in arctic soil profiles. *Soil Biol. Biochem.* **88**, 236–246 (2015).
20. Xu, X., Sherry, R. A., Niu, S., Zhou, J. & Luo, Y. Long-term experimental warming decreased labile soil organic carbon in a tallgrass prairie. *Plant Soil* **361**, 307–315 (2012).
21. Broder, T., Blodau, C., Biester, H. & Knorr, K. H. Peat decomposition records in three pristine ombrotrophic bogs in southern Patagonia. *Biogeosciences* **9**, 1479–1491 (2012).
22. Adamczyk, M., Perez-Mon, C., Gunz, S. & Frey, B. Strong shifts in microbial community structure are associated with increased litter input rather than temperature in High Arctic soils. *Soil Biol. Biochem.* **151**, 108054 (2020).
23. Hug, L. A. et al. Community genomic analyses constrain the distribution of metabolic traits across the Chloroflexi phylum and indicate roles in sediment carbon cycling. *Microbiome* **1**, 22 (2013).
24. Yun, J. L., Ju, Y. W., Deng, Y. C. & Zhang, H. X. Bacterial community structure in two permafrost wetlands on the Tibetan Plateau and Sanjiang Plain, China. *Microb. Ecol.* **68**, 360–369 (2014).
25. Zhong, Q. et al. Water table drawdown shapes the depth-dependent variations in prokaryotic diversity and structure in Zoige peatlands. *FEMS Microbiol. Ecol.* https://doi.org/10.1093/femsec/fix049 (2017).
26. Karhu, K. et al. Temperature sensitivity of soil respiration rates enhanced by microbial community response. *Nature* **513**, 81–84 (2014).
27. Thiessen, S., Gleixner, G., Wutzler, T. & Reichstein, M. Both priming and temperature sensitivity of soil organic matter decomposition depend on microbial biomass – An incubation study. *Soil Biol. Biochem.* **57**, 739–748 (2013).
28. Walker, T. W. N. et al. Microbial temperature sensitivity and biomass change explain soil carbon loss with warming. *Nat. Clim. Chang.* **8**, 885–899 (2018).
29. Dungait, J. A. J., Hopkins, D. W., Gregory, A. S. & Whitmore, A. P. Soil organic matter turnover is governed by accessibility not recalcitrance. *Glob. Chang. Biol.* **18**, 1781–1796 (2012).

30. Conant, R. T. et al. Temperature and soil organic matter decomposition rates - synthesis of current knowledge and a way forward. *Global Chang. Biol.* **17**, 3392–3404 (2011).

31. Hietz, P. et al. Long-term change in the nitrogen cycle of tropical forests. *Science* **4**, 334 (2011).

32. Manzoni, S., Taylor, P., Richter, A., Porporato, A. & Agren, G. I. Environmental and stoichiometric controls on microbial carbon-use efficiency in soils. *New Phytol.* **196**, 79–91 (2012).

33. Sistla, S. A., Asao, S. & Schimel, J. P. Detecting microbial N-limitation in tussock tundra soil: Implications for Arctic soil organic carbon cycling. *Soil Biol. Biochem.* **55**, 78–84 (2012).

34. Chen, L. et al. Nitrogen availability regulates topsoil carbon dynamics after permafrost thaw by altering microbial metabolic efficiency. *Nat. Commun.* **9**, 3951 (2018).

35. Soong, J. L. et al. Five years of whole-soil warming led to loss of subsoil carbon stocks and increased CO_2 efflux. *Sci. Adv.* **7**, eabd1343 (2021).

36. Chen, L. et al. Determinants of carbon release from the active layer and permafrost deposits on the Tibetan Plateau. *Nat. Commun.* **7**, 13046 (2016).

37. Girkin, N. T. et al. Interactions between labile carbon, temperature and land use regulate carbon dioxide and methane production in tropical peat. *Biogeochemistry* **147**, 87–97 (2019).

38. Swails, E. et al. Will CO_2 emissions from drained tropical peatlands decline over time? Links between soil organic matter quality, nutrients, and C mineralization rates. *Ecosystems* **21**, 868–885 (2017).

39. Ismawi, S., Gandaseca, S. & Ahmed, O. Effects of deforestation on soil major macro-nutrient and other selected chemical properties of secondary tropical peat swamp forest. *Int. J. Phys. Sci.* **7**, 2225–2228 (2012).

40. Kimura, S., Melling, L. & Goh, K. Influence of soil aggregate size on greenhouse gas emission and uptake rate from tropical peat soil in forest and different oil palm development years. *Geoderma* **185**, 1–5 (2012).

41. Takakai, F. et al. Effects of agricultural land-use change and forest fire on N_2O emission from tropical peatlands, Central Kalimantan, Indonesia. *Soil Sci. Plant Nutr.* **52**, 662–674 (2006).

42. Knoblauch, C., Beer, C., Sosnin, A., Wagner, D. & Pfeiffer, E. M. Predicting long-term carbon mineralization and trace gas production from thawing permafrost of Northeast Siberia. *Glob. Chang. Biol.* **19**, 1160–1172 (2013).

43. Treat, C. C. et al. Temperature and peat type control CO_2 and CH_4 production in Alaskan permafrost peats. *Glob. Chang. Biol.* **20**, 2674–2686 (2014).

44. Hobbie, S. E., Schimel, J. P., Trumbore, S. E. & Randerson, J. Controls over carbon storage and turnover in high-latitude soils. *Glob. Chang. Biol.* **6**, 196–210 (2000).

45. Keller, J. K., Bauers, A. K., Bridgham, S. D., Kellogg, L. E. & Iversen, C. M. Nutrient control of microbial carbon cycling along an ombrotrophic-minerotrophic peatland gradient. *J. Geophys. Res.* https://doi.org/10.1029/2005jg000152 (2006).

46. Chen, H. et al. A historical overview about basic issues and studies of mires (in Chinese). *Sci. Sin.* **51**, 15–26 (2020).

47. Ridl, J. et al. Plants rather than mineral fertilization shape microbial community structure and functional potential in legacy contaminated soil. *Front. Microbiol.* **7**, 1–10 (2016).

48. Kane, E. S. et al. Response of anaerobic carbon cycling to water table manipulation in an Alaskan rich fen. *Soil Biol. Biochem.* **58**, 50–60 (2013).

49. Carrell, A. A. et al. Experimental warming alters the community composition, diversity, and N_2 fixation activity of peat moss (Sphagnum fallax) microbiomes. *Glob. Chang. Biol.* **25**, 2993–3004 (2019).

50. Lamit, L. J. et al. Patterns and drivers of fungal community depth stratification in Sphagnum peat. *FEMS Microbiol. Ecol.* **93**, fix082 (2017).

51. Harrison, R. B., Footen, P. W. & Strahm, B. D. Deep soil horizons: contribution and importance to soil carbon pools and in assessing whole-ecosystem response to management and global change. *Forest Sci.* **57**, 67–76 (2011).

52. Krüger, J. P., Leifeld, J., Glatzel, S., Szidat, S. & Alewell, C. Biogeochemical indicators of peatland degradation – a case study of a temperate bog in northern Germany. *Biogeosciences* **12**, 2861–2871 (2015).

53. Franzén, L. G. Increased decomposition of subsurface peat in Swedish raised bogs: are temperate peatlands still net sinks of carbon? *Mires Peat* **1**, 3 (2006).

54. Eilers, K. G., Lauber, C. L., Knight, R. & Fierer, N. Shifts in bacterial community structure associated with inputs of low molecular weight carbon compounds to soil. *Soil Biol. Biochem.* **42**, 896–903 (2010).

55. de Graaff, M. A., Jastrow, J. D., Gillette, S., Johns, A. & Wullschleger, S. D. Differential priming of soil carbon driven by soil depth and root impacts on carbon availability. *Soil Biol. Biochem.* **69**, 147–156 (2014).

56. Peay, K. G., Kennedy, P. G. & Brun, T. D. Fungal community ecology: a hybrid beast with a molecular master. *BioScience* **58**, 799–810 (2008).

57. Gillabel, J., Cebrian, B., Six, J. & Merckx, R. Experimental evidence for the attenuating effect of SOM protection on temperature sensitivity of SOM decomposition. *Glob. Chang. Biol.* **16**, 2789–2798 (2010).

58. Pries, C. E. H., Castanha, C., Porras, R. C. & Torn, M. S. The whole-soil carbon flux in response to warming. *Science* **355**, 1420–1423 (2017).

59. Hicks Pries, C. E., Schuur, E. A. G. & Crummer, K. G. Thawing permafrost increases old soil and autotrophic respiration in tundra: partitioning ecosystem respiration using $\delta^{13}C$ and $\Delta^{14}C$. *Global Chang. Biol.* **19**, 649–661 (2013).

60. Tian, J. et al. Aerobic environments in combination with substrate additions to soil significantly reshape depth-dependent microbial distribution patterns in Zoige peatlands, China. *Appl.Soil Ecol.* **170**, 104252 (2022).

61. Feng, W. et al. Enhanced decomposition of stable soil organic carbon and microbial catabolic potentials by long-term field warming. *Glob. Chang. Biol.* **00**, 1–12 (2017).

62. Feng, W. et al. Methodological uncertainty in estimating carbon turnover times of soil fractions. *Soil Biol. Biochem.* **100**, 118–124 (2016).

63. Liang, J. et al. Methods for estimating temperature sensitivity of soil organic matter based on incubation data: A comparative evaluation. *Soil Biol. Biochem.* **80**, 127–135 (2015).

64. Cai, A., Feng, W., Zhang, W. & Xu, M. Climate, soil texture, and soil types affect the contributions of fine-fraction-stabilized carbon to total soil organic carbon in different land uses across China. *J. Environ. Manag.* **172**, 2–9 (2016).

65. Liu, L. et al. Response of anaerobic mineralization of different depths peat carbon to warming on Zoige plateau. *Geoderma* **337**, 1218–1226 (2019).

66. Waldrop, M. et al. Molecular investigations into a globally important carbon pool: permafrost protected carbon in Alaskan soils. *Glob. Chang. Biol.* **16**, 2543–2554 (2014).

67. Mooshammer, M., Wanek, W., Zechmeister-Boltenstern, S. & Richter, A. Stoichiometric imbalances between terrestrial decomposer communities and their resources: mechanisms and implications of microbial adaptations to their resources. *Front. Microbiol.* **5**, 22 (2014).

68. Blagodatskaya, E. & Kuzyakov, Y. Mechanisms of real and apparent priming effects and their dependence on soil microbial biomass and community structure: critical review. *Biol. Fertil. Soils* **45**, 115–131 (2008).

69. Chen, H. et al. The carbon stock of alpine peatlands on the Qinghai–Tibetan Plateau during the Holocene and their future fate. *Quat. Sci. Rev.* **95**, 151–158 (2014).

70. Sun, G. A study on the mineral formation law, classification and reserves of the peat in the Rouergai Plateau. *J. Nat. Res.* **7**, 334–345 (1992).

71. Liu, L. et al. Responses of peat carbon at different depths to simulated warming and oxidizing. *Sci. Total Environ.* **548-549**, 429–440 (2016).

72. Liu, L. et al. Water table drawdown reshapes soil physicochemical characteristics in Zoige peatlands. *Catena* **170**, 119–128 (2018).

73. Liu, L. et al. Carbon stock stability in drained peatland after simulated plant carbon addition: Strong dependence on deeper soil. *Sci. Total Environ.* **848**, 157539 (2022).

74. Yang, Z. et al. Soil properties and species composition under different grazing intensity in an alpine meadow on the eastern Tibetan Plateau, China. *Environ. Monit. Assess* **188**, 678 (2016).

75. Simpson, M. J. & Simpson, A. J. The chemical ecology of soil organic matter molecular constituents. *J. Chem. Ecol.* **38**, 768–784 (2012).

76. Lalonde, K., Mucci, A., Ouellet, A. & Gelinas, Y. Preservation of organic matter in sediments promoted by iron. *Nature* **483**, 198–200 (2012).

77. Deforest, J. L., zak, D. R., Pregitzer, K. S. & Burtonf, A. J. Atomspheric nitrate deposition and enhanced dissolved organic carbon leaching: test of a potential mechanism. *Soil Sci. Soc. Am. J.* **69**, 1233–1237 (2005).

78. Schadel, C. et al. Circumpolar assessment of permafrost C quality and its vulnerability over time using long-term incubation data. *Glob. Chang. Biol.* **20**, 641–652 (2014).

79. Bell, M. & Lawrence, D. Soil carbon sequestration - myths and mysteries. *Department of Primary Industries and Fisheries, Queensland Government* (2009).

80. Schadel, C., Luo, Y., David Evans, R., Fei, S. & Schaeffer, S. M. Separating soil CO_2 efflux into C-pool-specific decay rates via inverse analysis of soil incubation data. *Oecologia* **171**, 721–732 (2013).

81. Caporaso, J. G. et al. Global patterns of 16S rRNA diversity at a depth of millions of sequences per sample. *Proc. Natl Acad. Sci. USA* **108**, 4516–4522 (2011).

82. Gardes, M. & Bruns, T. D. ITS primers with enhanced specificity for basidiomycetes - application to the identification of mycorrhizae and rusts. *Mol. Ecol.* **2**, 113–118 (1993).

83. White, T. J. in *PCR-Protocols: A Guide to Methods and Applications* (Academic Press, 1990).

84. Bell, C. et al. High-throughput fluorometric measurement of potential soil extracellular enzyme activities. *J. Vis. Exp.* **81**, e50961 (2013).

85. DeForest, J. L. The influence of time, storage temperature, and substrate age on potential soil enzyme activity in acidic forest soils using MUB-linked substrates and L-DOPA. *Soil Biol. Biochem.* **41**, 1180–1186 (2009).

86. Amundson, R. The carbon budget in soils. *Annu. Rev. Earth Planet. Sci.* **29**, 535–562 (2001).
87. Trumbore, S. E. Potential responses of soil organic carbon to global environmental change. *Proc. Natl Acad. Sci. USA* **94**, 8284–8291 (1997).
88. R Core Team. R: a language and environment for statistical computing. *R Foundation for Statistical Computing.* https://www.r-project.org (2017).
89. Oksanen, J. et al. vegan: community ecology package. *R Packag version 24-1* (2016).
90. Asshauer, K. P., Wemheuer, B., Daniel, R. & Meinicke, P. Tax4Fun: predicting functional profiles from metagenomic 16S rRNA data. *Bioinformatics* **31**, 2882–2884 (2015).

Author contributions
H.C. and L.L. conceptualized the idea and designed this research; L.L. collected field samples, conducted incubation, and analyzed soil chemistry; J.T. did microbial experiments; L.L., H.C., and J.T. wrote and discussed the results of the manuscript.

Competing interests
The authors declare no competing interests.

Additional information
Supplementary information The online version contains supplementary material available at https://doi.org/10.1038/s43247-022-00651-y.

Correspondence and requests for materials should be addressed to Huai Chen.

Peer review information *Communications Earth & Environment* thanks the anonymous reviewers for their contribution to the peer review of this work. Primary Handling Editors: Clare Davis.

Reprints and permission information is available at http://www.nature.com/reprints

Publisher's note Springer Nature remains neutral with regard to jurisdictional claims in published maps and institutional affiliations.